Hyperbolic Shock Waves of the Optical Self-Focusing with Normal Group-Velocity Dispersion

L. Bergé,[1] K. Germaschewski,[2] R. Grauer,[2] and J. Juul Rasmussen[3]

[1]*Département de Physique Théorique et Appliquée, CEA/DAM–Ile de France, B.P. 12, F-91680 Bruyères-le-Châtel, France*
[2]*Lehrstuhl für Theoretische Physik I, Ruhr-Universität-Bochum, Universitätsstraße 150, D-44780 Bochum, Germany*
[3]*Optics and Fluids Dynamics Department, Risø National Laboratory, P.O. Box 49, DK-4000 Roskilde, Denmark*

(Received 21 December 2001; revised manuscript received 27 March 2002; published 24 September 2002)

The theory of focusing light pulses in Kerr media with normal group-velocity dispersion in (2 + 1) and (3 + 1) dimensions is revisited. It is shown that pulse splitting introduced by this dispersion follows from shock fronts that develop along hyperbolas separating the region of transverse self-focusing from the domain of temporal dispersion. Justified by a self-similar approach, this property is confirmed by numerical simulations using an adaptive-mesh refinement code.

DOI: 10.1103/PhysRevLett.89.153902 PACS numbers: 42.65.Jx, 41.20.Jb, 42.25.Bs

The propagation of ultrashort pulses in matter has become a topic of intense research, stimulated by the rapid progress of femtosecond laser sources. For instance, laser beams with a duration of about 100 fs form robust light channels in various transparent media [1], which result from the competition between the Kerr response of the material and other processes able to limit the intensity growth caused by self-focusing [2]. Among those, multiphoton ionization (MPI) [1], nonparaxiality [3], and temporal dispersion including group-velocity dispersion (GVD), space-time focusing, and self-steepening [3–7] have been proposed. While MPI applies to pulses capable of reaching peak intensities larger than 10^{13} W/cm^2, nonparaxiality comes into play when the beam size becomes comparable with the laser wavelength, λ_0. Thus, for pulses undergoing moderate intensity growths and waist compressions [5,6], temporal dispersion appears as an efficient candidate for inhibiting the collapse. In that case, the envelope $\psi(\vec{r}, t)$ of an optical pulse traveling at the group velocity v_g, with central frequency ω_0 and wave number $k(\omega_0)$, is currently modeled by the extended nonlinear Schrödinger (NLS) equation

$$i\partial_z\psi + T^{-1}\Delta_\perp\psi - \sigma\partial_t^2\psi + T(|\psi|^2\psi) = 0, \qquad (1)$$

where the coordinates (x, y) entering the transverse Laplacian, the retarded time t, the axial propagation distance z, and the intensity $|\psi|^2$ are normalized to the beam waist w_0, the pulse temporal half-width t_p, $2k(\omega_0)w_0^2$, and $\lambda_0^2/8\pi^2 w_0^2 n_0 n_2$, respectively ($n_0$ and n_2 are the linear and nonlinear refraction indices). Consistently, $\sigma = k(\omega_0)w_0^2\partial_\omega^2 k(\omega)|_{\omega_0}/t_p^2$ refers to the GVD coefficient. The operator $T \equiv 1 + (i/\omega_0 t_p)\partial_t$ in front of the cubic nonlinearity accounts for self-steepening and T^{-1} in front of the diffraction term $\Delta_\perp\psi$ for space-time focusing [6].

In the limit $T \to 1$, when the input beam power $P \equiv \int |\psi|^2 d\vec{r}$ is above the critical value $P_{\rm cr} \simeq 11.7$, solutions to Eq. (1) with $\sigma = 0$ can become singular at a finite distance, z_c [2]. With $\sigma > 0$, the nonlinearity, however, causes defocusing in time in addition to transverse focusing, which results in the splitting of the pulse and limits the collapse [4,5]. Reduced systems of partial differential equations [3] indicated that GVD defocuses the pulse around $t \simeq 0$, which creates two symmetric spikes along the temporal direction. In [7], a two-scale self-similar analysis also displayed evidence of the existence of two caustics along time, where the wave field formed two maxima. Earlier, it was conjectured [8] that, as the two peaks continue to self-focus, they could repeatedly split into symmetric subpeaks until the power P goes below $P_{\rm cr}$. However, this scenario of "multiple splitting" has not been observed clearly as yet. Instead, numerical simulations using an adaptive-mesh refinement (AMR) code showed that the interplay between self-focusing and GVD leads to the generic formation of temporal shocks at the peak edges [9]. Beyond the shock, the two peaks disintegrate into ripplelike cells, which, although they may partly self-focus, do not produce symmetric secondary peaks.

These shock structures have received no theoretical explanation, which is the issue of this Letter. The key idea is to reformulate Eq. (1) in hyperbolic coordinates $\eta^2 \equiv r^2 - t^2/\sigma$ ($r^2 = x^2 + y^2$), in order to describe the shock fronts emerging between focusing ($\eta^2 > 0$) and defocusing ($\eta^2 < 0$) regions in the (r, t) plane. Setting $T = 1$, we shall apply this new coordinate system to the (2 + 1)-dimensional Eq. (1), for which $\Delta_\perp = \partial_x^2$, and to the (3 + 1)-dimensional case, where $\Delta_\perp = r^{-1}\partial_r r\partial_r + r^{-2}\partial_\theta^2$. Splitting patterns in the (2 + 1)-dimensional Eq. (1) were recently analyzed by means of similar variables [10] and interpreted in terms of modulational instability of plane waves. Here, we show that the field sharply localizes near hyperbolas, whose number increases with the domain of the self-focusing core of $|\psi|$ along the direction η. In (3 + 1) dimensions, mainly one hyperbolic shock front arises, which is confirmed by 3D numerical simulations. Although discarded throughout the coming analysis, the role of the operators T, T^{-1} will briefly be discussed at the end of this Letter.

To start with, we pass over to the hyperbolic system of coordinates $\eta = \sqrt{r^2 - t^2/\sigma}$, $\mu = rt\cos\theta/\sqrt{\sigma}$, and

$\nu = rt\sin\theta/\sqrt{\sigma}$, which transforms Eq. (1) with $T = 1$ as

$$i\partial_z\psi + \eta^{1-d}\partial_\eta\eta^{d-1}\partial_\eta\psi + F(\partial_\mu\psi) + |\psi|^2\psi = 0. \quad (2)$$

Here, d refers to the space dimension number 2 in the $(2+1)$-dimensional case and $d = 3$ in the $(3+1)$-dimensional one. For technical convenience, we ignore the variations of ψ with respect to ν ($\theta = 0$). The function $F(\partial_\mu\psi)$ in Eq. (2) then involves μ derivatives as $F(\partial_\mu\psi) = (4\mu/\eta)\partial^2_{\mu\eta}\psi - \eta^2\partial^2_\mu\psi$. Equation (2) shows that, for initial distributions $\psi_0 \equiv \psi(\eta, \mu, 0)$ with weak dependence on μ, the main dynamics is embarked in the competition between $\eta^{1-d}\partial_\eta\eta^{d-1}\partial_\eta\psi$ and $|\psi|^2\psi$. This triggers a collapse dynamics, along which the η component of ψ tends to a self-similar shape. We therefore apply the separation of variables

$$\psi = u(\eta, z) \times v(\mu, z), \quad (3)$$

where the self-focusing component $u(\eta, z)$ is assumed to obey Eq. (2) with $F = 0$. Under this condition, $u(\eta, z)$ adopts the self-similar behavior

$$u(\eta, z) = L^{-1}(z)\phi(\xi, \zeta)e^{i\lambda\zeta(z) - i\beta(z)\xi^2/4}, \quad (4)$$

where $\xi = \eta/L(z)$, $\zeta(z) \equiv \int_0^z du/L^2(u)$, $\beta = -LL_z$, and the mean size of the beam along the η direction, $L(z)$, vanishes near focus. The new eigenfunction ϕ is expected to become self-similar in the sense that $\partial_\zeta\phi \to 0$. Following standard procedures [2,3,11], ϕ thus decomposes at leading order ($\beta_\zeta \to 0$) into core and tail parts as

$$\phi \simeq \phi_c(\xi)H(|\xi_T| - \xi) + C(\beta)\frac{e^{i\beta(z)\xi^2/4}}{\xi^{1+i\lambda/\beta}}H(\xi - |\xi_T|), \quad (5)$$

where $\xi_T \equiv (2/\beta)\sqrt{\lambda + i\beta(d/2 - 1)}$ and $H(x)$ denotes the Heaviside function. The core distribution ϕ_c extends in the bounded domain $\xi < |\xi_T|$ only. Its shape is close to the ground-state solution ϕ_0 obeying $-\lambda\phi_0 + \Delta_\xi\phi_0 + \phi_0^3 = 0$, whose best fit is provided by the sech function

$$\phi_0(\xi) \simeq A\cosh^{-1}(\xi/a), \quad (6)$$

with appropriate amplitude A and width a [12].

Next, after introducing Eq. (3) into Eq. (2) and averaging the resulting equation over the u component, we rewrite $v(\mu, z)$ in terms of self-similar variables as $v = Q(\rho, \zeta)$ with $\rho = \mu/L^2$. We find that Q satisfies

$$i\partial_\zeta Q - 4\alpha\rho\partial_\rho Q - \delta\partial^2_\rho Q + \gamma(|Q|^2 - 1)Q = 0, \quad (7)$$

where $\alpha \equiv -\langle\xi^{-1}\phi^*\partial_\xi\phi\rangle$, $\delta \equiv \langle\xi^2|\phi|^2\rangle$, and $\gamma \equiv \langle|\phi|^4\rangle$, with $\langle f\rangle \equiv \int f d\vec{\xi}/\int|\phi|^2 d\vec{\xi}$ are evaluated with Eq. (6). In self-similar regimes, we assume $\partial_\zeta Q \to 0$, so that $Q(\rho)$ behaves as a dark soliton at center $\rho \sim 0$ and decays to zero for $\rho \gg 1$. $Q(\rho)$ follows the approximation

$$Q(\rho) \simeq \tanh(\rho/\sqrt{\delta})H(\rho_c - \rho) + \frac{C'}{\rho^{\gamma/4\alpha}}H(\rho - \rho_c), \quad (8)$$

with $\rho_c \approx \sqrt{\delta/4\alpha}$, where the constant C' is fixed by solving numerically Eq. (7) with $\partial_\zeta Q = 0$.

Let us now emphasize the key dynamics underlying the shock formation. For small enough ξ, the solution ϕ becomes close to the core ϕ_c and u converges to $u_c = L^{-1}\phi_c e^{i\lambda\zeta - i\beta\xi^2/4}$. Near the boundary $\eta^2 = 0$, this solution must, by continuity, be identical in the focusing and defocusing regions as well. From expression (6), u then behaves like $L^{-1}(z)A/\cos[\sqrt{t^2/\sigma - r^2}/aL(z)]$ as $\eta^2 \to 0$ from below. Thus, in the domain $\eta^2 \le 0$, the core solution develops singularities issued from poles distributed along the hyperbolas $t^2/\sigma - r^2 = \eta_c^2 = \frac{\pi^2}{4}a^2L^2(z)(2n+1)^2$, with n being an integer. Hyperbolas of poles represent shock fronts between the focusing and defocusing regions and for a fixed boundary, e.g., $|\eta| < 1$, their number increases as $L(z)$ decreases. Near the focus, z_c, $(n+1)$ hyperbolas of spiky fields are excited inside the core domain bounded by $|\eta| < |\eta_T| \equiv |\xi_T|L(z)$. Hence, the number of hyperbolas is limited to

$$n + 1 < |\xi_T|/\pi a + 1/2. \quad (9)$$

We now determine these singular profiles for the cases $d = 2$ and $d = 3$, separately.

(2 + 1)-dimensional shock profiles.—For $d = 2$, self-focusing follows the route of a "strong" collapse [2,13]. The function β satisfies $\beta_\zeta \sim e^{-\pi\lambda/\beta} \sim C^2(\beta)$ with $\lambda = 1$ and tends logarithmically to zero as $\zeta \to +\infty$. With decreasing $\beta < 1$, the core extension domain $\xi_T = 2/\beta$ slowly increases and the core solution thus tends to ϕ_0, modeled by Eq. (6) with $A = \sqrt{12\ln 2/(4\ln 2 - 1)} \simeq 2.17$ and $a = \sqrt{2\ln 2 + 1}/\sqrt{6\ln 2} \simeq 0.76$ [12]. By choosing the typical mean values $\beta = 0.25$–0.3 that precede the establishment of an effective collapse singularity for, e.g., Gaussian beams [11], Eq. (9) predicts that three hyperbolas should form at maximum compression.

Figure 1 compares direct numerical simulations of Eq. (1) using the AMR code described in [9] with 3D plots of the analytical solution (3) for $\sigma = +1$. We have used the same initial condition $\psi_0 = (A_0/\eta_0)e^{-\eta^4/2\eta_0^4 - \mu^2/2\mu_0^2}$ with $A_0 = 25$, $\eta_0 = 3$, and $\mu_0 = 3.5$ as that employed in [10]. We also simulated Gaussian beams, whose evolution was qualitatively the same, apart from two primary peaks arising in the early stage. At $z = 0.12$, wave compression first forms two symmetric shock fronts when $L(z) \sim \eta_0/3$ [Fig. 1(a)]. At larger $z \to z_c = 0.19$, several hyperbolas emerge as the mean size of the pulse decreases to the lowest value $L(z) \sim \eta_0/10$ [Fig. 1(b)]. These hyperbolas neither take place in the plane $\eta^2 > 0$ nor undergo modulational instability. Instead, they form in the inner domain $\eta^2 \le 0$ along which split pulses are emitted. Figure 1(c) restores this stage. Plotted from Eq. (3) with the scale length $L(z) = 0.3$ and $\beta = 0.3$, it shows diverging spikes distributed along hyperbolas, whose sharp maxima are damped by the μ derivatives of Eq. (2). The component $v = Q(\mu/L^2, \zeta)$ indeed limits the divergence of (3) by digging

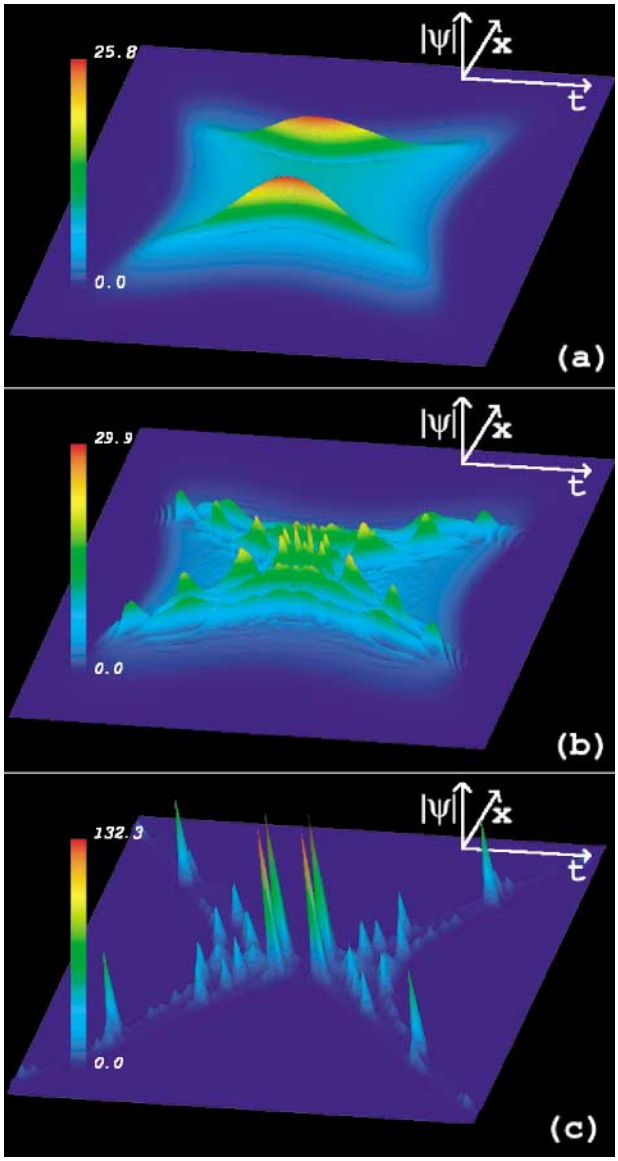

FIG. 1 (color). (a) $|\psi|$ vs (x, t) at $z = 0.12$ from numerical integration of Eq. (1) for $d = 2$, $\sigma = +1$, and fourth-order super-Gaussian initial condition. (b) $|\psi|$ at $z \simeq z_c = 0.19$. (c) $|\psi| = |u| \times |v|$ vs (x, t) constructed from Eq. (3), where u and v are given by the combination of Eqs. (4), (5), and (8), with ϕ_c defined by its sech approximation and $L = \beta = 0.3$. Patterns are centered around $x = t = 0$.

a hole at the center and by localizing $|\psi|$ at large r and t. The constants in Eq. (7) take the values $\alpha = 1.3$, $\delta = 1.18$, and $\gamma = 2$, and the function Q, once computed numerically, is evaluated by Eq. (8) with $C' \simeq 0.46$. Note that around center the analytical estimate $|\psi| = L^{-1}|\phi| \times |Q|$ promotes singularities that we soften by using a limited resolution in Fig. 1(c). These poles actually result from the assumption of exact self-similarity, which we apply to our model, but is never strictly attained in Eq. (1). From this representation of $|\psi|$, we shall retain that transverse compression pushes the boundary layer $|\eta_c| = (2n + 1)\pi a L(z)/2$ separating focusing/defocusing domains to zero, which excites hyperbolic shock waves with diverging spikes. The number of shock fronts increases as $L(z) \to 0$, but remains limited by the extension domain of the core, $|\eta| < |\eta_T|$. On the whole, Fig. 1 emphasizes the occurrence of three hyperbolic shock waves at maximal compression, as expected.

(3 + 1)-dimensional shock profiles.—For $d = 3$, collapsing solutions shrink with a scale length $L(z) \sim (z_c - z)^{1/2}$, according to the "weak" collapse scenario [13]; i.e., collapse becomes rapidly self-similar and the function ϕ recovers a universal localized shape characterized by $\lambda = 0.545$ and $\phi(0) = 1.39$, whenever β is fixed to $1/2$. This self-similar state (5) has a core distribution close to Eq. (6) in the central domain $\xi < |\xi_T| \simeq 3.1$, and close to the decreasing tail $\phi_T \simeq C/\xi^{1+2i\lambda}$ with $C^2 = 2.02$ in the outer region $\xi > |\xi_T|$. The core ϕ_c is again modeled by Eq. (6), in which imposing $A = \phi(0) = 1.39$ requires one to tune suitably the soliton width to $a = a'A'/\phi(0) = 1.4$. Here, $a' = \sqrt{\pi^2 + 12}/3\pi$ and $A' = \sqrt{6\pi^2/(\pi^2 - 6)}$ are the amplitude and size of a 3D NLS soliton with $\lambda = 1$. Near the boundary $r \simeq t/\sqrt{\sigma}$, shock fronts arise along the hyperbolas defined by Eq. (9), where $a \simeq 1.4$. As in the 2D case, the number of hyperbolas increases all the more as $L(z)$ becomes smaller, but it is still limited by the core extension domain $|\eta| < |\eta_T|$ near focus. The main difference lies in the values of the size parameter a and in the self-similar value of the turning point $|\xi_T|$, which are, respectively, twice longer and smaller than their two-dimensional counterparts. As a result, the number of hyperbolas diminishes compared with the 2D case. With $\beta = 0.5$, only one hyperbola of spikes is excited. This may justify why multipeaked structures, which should be distributed along distinct hyperbolas, are absent from the shock patterns revealed in Ref. [9].

Figure 2(a) exhibits the amplitude $|\psi|$ versus $(x, y = 0, t)$ numerically integrated from Eq. (1) in $(3 + 1)$ dimensions with the Gaussian datum, $\psi_0 = A_0 e^{-(x^2+y^2)/2-t^2/2}$, where $A_0 = 3.6$ ($P = 3.5 P_{\rm cr}$). We also used 3D super-Gaussianlike initial conditions of similar power, which restored the same dynamics. Maximal compression is attained as the ratio $L(z)/L(0)$ reaches 0.1–0.15. For comparison, Fig. 2(b) shows a 3D plot of $|\psi|$ modeled by Eq. (3) with $L(z) = 0.15$ and $\beta = 1/2$ that reproduces the splitting pattern of Fig. 2(a). The averaging coefficients in Eq. (7) take the values $\alpha \simeq 0.35$, $\delta \simeq 3.7$, and $\gamma \simeq 0.64$, and the function Q, constrained to the self-similar limit, behaves closely to Eq. (8), where $C' \simeq 3.17$. On the whole, only one hyperbolic shock front forms, as expected. Figure 2(c) then shows the further numerical evolution of the shock disintegration into ripplelike cells distributed along hyperboloids after the focus. Because it only involves the self-similar limit of $|\psi|$ near the point z_c of maximum compression, our modeling cannot reproduce these secondary cells. We can, however, anticipate that the transition from a self-compression regime ($L_z < 0$) to a dispersive one ($L_z > 0$) will force the function β to decrease at some distance $z > z_c$, which would allow,

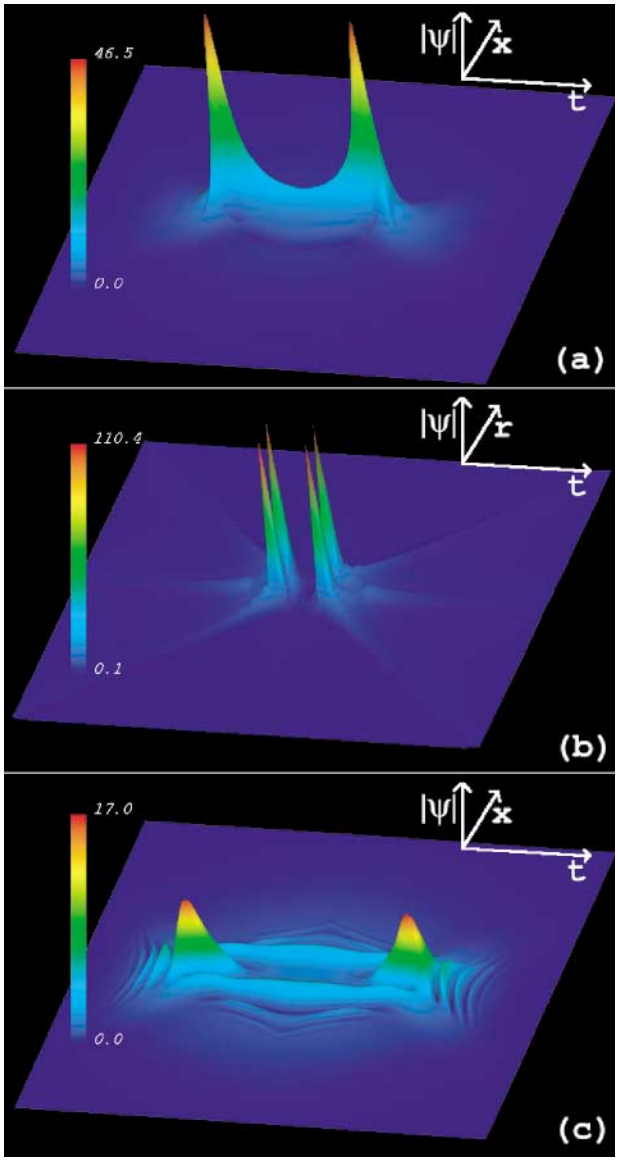

FIG. 2 (color). (a) $|\psi|$ vs $(x, 0, t)$ from AMR numerical simulation of Eq. (1) for $\sigma = +1$ and $d = 3$ at $z \simeq z_c = 0.26$ ($\psi_0 =$ Gaussian). (b) Analytical representation of $|\psi| = |u| \times |v|$ vs (r, t) with $L(z) = 0.15$ and $\beta = 0.5$. (c) Formation of ripplelike cells as the pulse spreads out at later $z = 0.2735$.

through the increase of $|\xi_T|$, for the formation of higher-order hyperbolas giving rise to ripplelike cells.

Let us now qualitatively comment on the influence expected from the operators T, T^{-1} in Eq. (1). Assuming $T^{-1} \simeq 1 - (i/\omega_o t_p)\partial_t$ as $\omega_0 t_p \gg 1$, their action can be evaluated from the equation for power

$$\partial_z P = \partial_t \int \left\{ 2\sigma |\psi|^2 \partial_t \arg(\psi) - \frac{1}{\omega_o t_p}\left(\frac{3}{2}|\psi|^4 + |\nabla_\perp \psi|^2\right)\right\} d\vec{r}, \qquad (10)$$

where the first integral term refers to GVD which creates two symmetric peaks. The last contribution involves time derivatives from T, T^{-1} applied to the L^4 norm and to the gradient norm of ψ, which both diverge in the collapse regime [2]. Starting from a bell-shaped pulse centered on $t = 0$, we infer that power will be transferred into the time region where $\partial_t |\psi|^2$ is negative and thus enhance the trailing peak emerging at $t > 0$. Self-steepening and space-time focusing should hence make the shock profiles asymmetric, which was experimentally reported in [6].

In summary, self-similar collapsing states have enabled us to describe the hyperbolic shock fronts taking place in the boundary layer separating focusing/defocusing domains in NLS equations with normal GVD. The shocks develop with singular spikes distributed along hyperbolas. In the $(2 + 1)$-dimensional case, several shock waves arise as the core solution of $|\psi|$ expands in a rather large region ($|\xi_T| = 2/\beta \gg 1$). This process generates a turbulent, multipeaked wave field. In the $(3 + 1)$-dimensional case, the self-focusing core exhibits a narrower extension domain ($|\xi_T| = 3.1$). One hyperbolic shock front forms, which provides the two-peaked profile discovered in [4].

[1] S. Tzortzakis *et al.*, Phys. Rev. Lett. **86**, 5470 (2001); **87**, 213902 (2001), and references therein.
[2] J. Juul Rasmussen and K. Rypdal, Phys. Scr. **33**, 481 (1986); L. Bergé, Phys. Rep. **303**, 259 (1998).
[3] G. Fibich and G. C. Papanicolaou, Phys. Rev. A **52**, 4218 (1995); SIAM J. Appl. Math. **60**, 183 (1999); see also G. G. Luther, A. C. Newell, and J. V. Moloney, Physica (Amsterdam) **74D**, 59 (1994).
[4] J. E. Rothenberg, Opt. Lett. **17**, 583 (1992); P. Chernev and V. Petrov, Opt. Commun. **87**, 28 (1992); Opt. Lett. **17**, 172 (1992).
[5] J. K. Ranka, R. W. Schirmer, and A. L. Gaeta, Phys. Rev. Lett. **77**, 3783 (1996); S. A. Diddams, H. K. Eaton, A. A. Zozulya, and T. S. Clement, Opt. Lett. **23**, 379 (1998).
[6] J. K. Ranka and A. L. Gaeta, Opt. Lett. **23**, 534 (1998); see also T. Brabec and F. Krausz, Phys. Rev. Lett. **78**, 3282 (1997); D. Homoelle and A. L. Gaeta, Opt. Lett. **25**, 761 (2000).
[7] L. Bergé *et al.*, J. Opt. Soc. Am. B **13**, 1879 (1996).
[8] N. A. Zharova *et al.*, JETP Lett. **44**, 13 (1986).
[9] K. Germaschewski *et al.*, Physica (Amsterdam) **151D**, 175 (2001).
[10] A. G. Litvak, V. A. Mironov, and E. M. Sher, Phys. Rev. E **61**, 891 (2000); JETP **91**, 1268 (2000).
[11] D. W. McLaughlin *et al.*, Phys. Rev. A **34**, 1200 (1986); N. E. Kosmatov, V. F. Shvets, and V. E. Zakharov, Physica (Amsterdam) **52D**, 16 (1991).
[12] D. Anderson, M. Bonnedal, and M. Lisak, Phys. Fluids **22**, 1838 (1979).
[13] V. E. Zakharov and E. A. Kuznetsov, Sov. Phys. JETP **64**, 773 (1986).